Exciton and Biexciton Fine Structure in Single Elongated Islands Grown on a Vicinal Surface

L. Besombes,* K. Kheng, and D. Martrou

CEA-Grenoble, Département de Recherche Fondamentale sur la Matière Condensée/SP2M, 17 avenue des Martyrs, 38054 Grenoble Cedex 9, France

(Received 24 March 2000)

We report a microphotoluminescence study of the exciton and the biexciton localized in very elongated islands formed by well-width fluctuations in a thin CdTe/CdMgTe quantum well grown on a vicinal surface. The electron-hole exchange interaction in a local reduced symmetry splits the exciton states. The resulting transitions are linearly polarized along the two orthogonal principal axes of the island. The valence band mixing induced by the elongated shape of the potential leads to a strong polarization anisotropy and to the observation of dark exciton states under magnetic field. The biexciton-exciton transition reproduces all the fine structure of the exciton state including the transition of the biexciton to the dark exciton state.

PACS numbers: 78.55.Et, 71.35.Ji, 71.70.Gm

Optical spectroscopy of single semiconductor quantum dots (QDs) is presently a very active field of basic physics studies. Three dimensionally confined excitons or excitonic complexes represent an important new class of model systems for studying fundamental physics at the nanometer scale. Although different fabrication techniques exist for artificial semiconductor structures, size and/or composition fluctuations still prevent the study of intrinsic properties of the low-dimensional system unless a high spatial and spectral resolution technique is used [1,2]. In narrow, high quality quantum wells, fluctuations at the interfaces lead to the localization of excitons in monolayer-high islands. These localized states can be regarded as weakly confined quantum dot states. One dimension of the confinement is defined by the width of the quantum well while the other two lateral dimensions are defined by the size of the island. In the present Letter we show that in such a structure the preparation of the substrate surface can be used to shape the lateral confinement potential.

We study in detail the fine structure and polarization properties of excitons and biexcitons confined in elongated CdTe islands formed on a CdMgTe vicinal surface. The formation of the biexciton [3,4], the effect of the exchange interaction on the exciton and biexciton fine structure, and the mixing of bright and dark exciton states under magnetic field are discussed [5]. The exciton zero field splitting and the observed anisotropy of linear polarization show clearly that highly asymmetric island structures with properties approaching those of quantum wires have been obtained.

The sample is a nominally 10 monolayers (3.2 nm) thick CdTe/$Cd_{0.72}Mg_{0.28}Te$ quantum well grown by atomic layer epitaxy (ALE) [6] on a (001) $Cd_{0.96}Zn_{0.04}Te$ substrate misoriented 1° toward ⟨100⟩ (a 1 °C vicinal surface). Scanning tunneling microscope (STM) studies of (001) CdTe vicinal surfaces have allowed us to determine efficient smoothing conditions for preparing the substrate [7]: After annealing at 330 °C under a Te flux, a 1 °C $Cd_{0.96}Zn_{0.04}Te$ vicinal surface shows 18 nm wide monomolecular steps parallel to the ⟨100⟩ direction, organized in a staircase array. In the present sample a growth interrupt was performed under these smoothing conditions after the growth of the first $Cd_{0.72}Mg_{0.28}Te$ barrier. The first interface of the well is then self-organized in a staircase array. Figure 1a shows the STM image of a CdTe 1 °C vicinal surface after a few ALE cycles on a smoothed surface: the staircase array is conserved but it becomes less regular. This should represent the morphology of the second CdTe/$Cd_{0.72}Mg_{0.28}Te$ interface. The monolayer well-width fluctuations are expected to

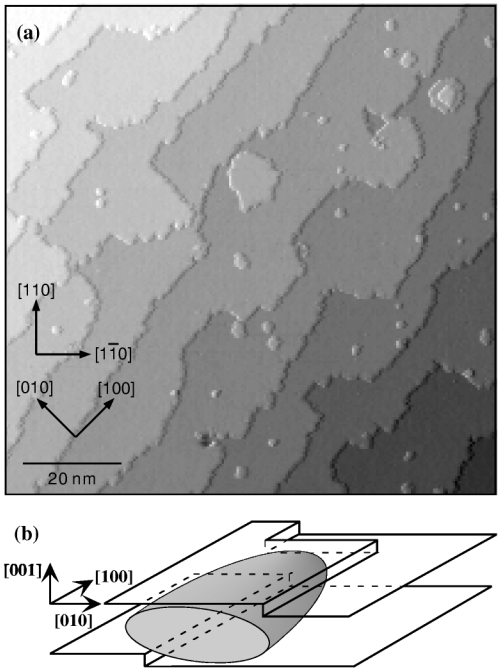

FIG. 1. (a) Representative scanning tunneling microscope image of a CdTe 1 °C vicinal surface. This image is obtained after a few ALE cycles at 310 °C on a smoothed surface. The surface presents monomolecular steps running along the ⟨100⟩ direction. (b) Schematic representation of the wave function of an exciton localized in the structure.

create a highly anisotropic lateral (in-plane) potential with symmetry axes oriented along the ⟨100⟩ axes (Fig. 1b).

To carry out microphotoluminescence (μ-PL) measurements we use electron beam lithography and metal lift-off to open a series of apertures in an opaque, 100 nm thick Al film deposited on the surface of the sample. The photoluminescence (PL) is excited by an Ar^+ laser and detected through the same aperture. The spatial resolution is defined in this manner by the size (20 to 0.3 μm) of the probed aperture. The spectral resolution of the experimental setup is 60 μeV in the spectral range considered in this paper.

The macro-PL spectra show a very broad (FWHM = 20 meV) excitonic line at 1817 meV. The inhomogeneous linewidth is consistent with the potential fluctuations induced by a one monolayer variation of the thin CdTe layer. On probing with the high spatial resolution, the broad PL peak resolves into a series of extremely sharp lines (FWHM = 100 μeV). The number of lines changes with the aperture size and the excitation power. However, at low excitation power (i.e., about 1 W/cm^2) each discrete line can be assigned to the recombination of a single exciton localized in an island formed by the interface fluctuations.

In the following, we discuss the low temperature (4 K) spectra taken from a 0.3 μm diameter aperture where only a few dominant single excitonic transitions are observed. Figure 2 shows the emission spectra for various excitation powers P_{exc}. At low excitation a luminescence line with a doublet structure, labeled X, dominates the spectra. It is attributed, as will be discussed later, to an exciton localized in an island and split by the electron-hole exchange interaction. The exciton line gains intensity linearly with P_{exc} and the spectra are normalized to its intensity. On increasing the excitation density, a peak labeled XX appears 7.2 meV below the exciton line. Its intensity increases superlinearly at low excitation and its doublet structure reproduces the spectral pattern of the exciton with the order of transitions reversed. For these reasons we assign this peak XX to the biexciton-exciton transition in the same island [8]. The lateral confinement in the thin CdTe layer leads to the accumulation of excitons in the lowest energy localization sites and so very strongly enhances the formation of the biexciton. The biexciton binding energy (7.2 meV) measured in this II-VI structure is enhanced as compared to that determined in equivalent III-V structures (about 4 meV [1,8]). This is a consequence of the stronger electron-hole correlation in a II-VI material. On the other hand, the biexciton binding energy reported for another type of II-VI structure where the excitonic effect is stronger, namely, CdSe/ZnSe QDs, is about 17 meV [4].

Both the exciton and the biexciton emissions consist of two Lorentzian lines split by 170 μeV, with about a 100 μeV linewidth (Figs. 3a and 3a′). The two components of each doublet are linearly polarized along two orthogonal axes, labeled Π_x and Π_y. The striking results are (i) the great difference in intensity between the two

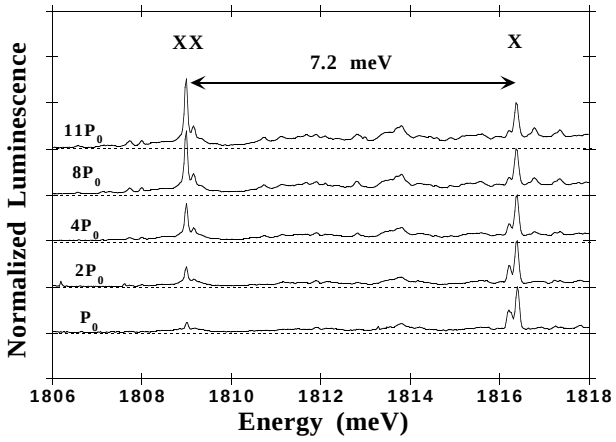

FIG. 2. Nonpolarized μ-PL spectra from a single island for different excitation powers. The spectra are taken from an aperture of about 300 nm diameter and normalized to the intensity of the exciton line (X). XX corresponds to the recombination of the biexciton ground state. P_0 is about 1 W/cm^2.

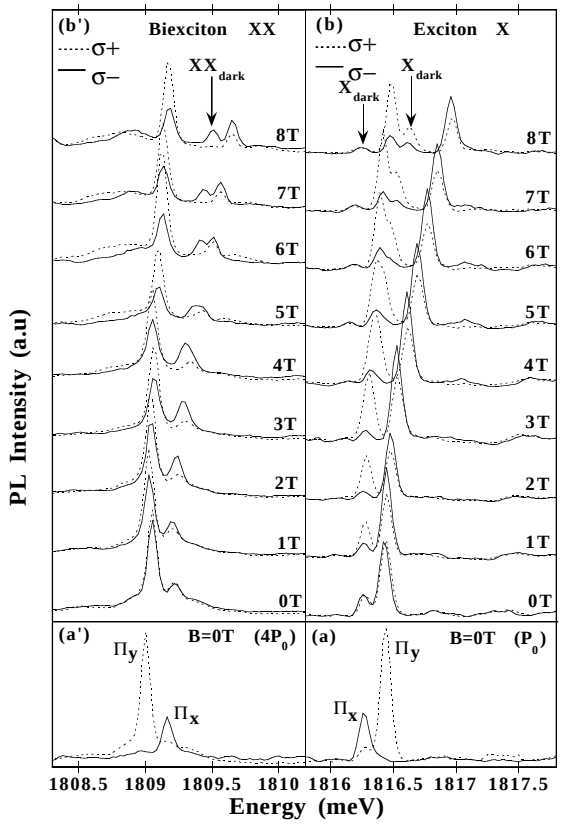

FIG. 3. (a),(a′) Linearly polarized PL spectra of a single island with reduced symmetry, at zero magnetic field. (b),(b′). Circularly polarized PL spectra ($\sigma-$ and $\sigma+$ in solid and dotted lines, respectively) for various magnetic fields increasing from bottom to top. Arrows point out the dark exciton states. The excitation power is P_0 for the X spectra (a),(b) and $4P_0$ for the XX spectra (a′),(b′). P_0 is about 1 W/cm^2. The PL at 0 T detected through a circular polarizer gives the real relative intensity of the emission components without the linear polarization response of the monochromator.

components of each doublet and (ii) the mirror symmetry of the sequence of the intensity and polarization between the X and XX transitions: the weaker component, polarized Π_x, is at lower energy for X and at higher energy for XX. Of course we have taken care to ensure that the difference in intensity is not an artifact of the experimental setup. Moreover, we found that one of the polarization directions is at 35° to the edge of the sample with an accuracy of about 5°. This direction roughly corresponds to one of the ⟨100⟩-equivalent crystallographic axes which are both exactly at 45° from the sample's cleaved edge.

These observations can be accounted for by the spin structure of X and XX. The residual biaxial strain in the CdTe layer and the quantum well confinement lifts the degeneracy between the heavy and light hole subbands. In a first approximation we can then consider that the observed transitions correspond to heavy-hole exciton states. The heavy-hole exciton in zinc blende based quantum wells (D_{2d} point group) is fourfold degenerate and characterized by the angular momentum components $M = \pm 1, \pm 2$. The electron-hole exchange interaction splits this quartet into the radiative doublet $|\pm 1\rangle$ and two close lying nonradiative singlets formed by a symmetric and an antisymmetric combinations of $|\pm 2\rangle$ states [9]. An anisotropic confinement potential in the well plane will reduce the point group symmetry and then will mix the $M = \pm 1$ exciton states. The radiative doublet is split into the states $\frac{1}{\sqrt{2}}(|+1\rangle \pm |-1\rangle)$ which are dipole active along the two orthogonal principal axes of the nanostructure (Fig. 4) [10,11]. So the observed directions of linear polarization, Π_x and Π_y, indicate that the excitons are localized in asymmetric islands elongated along the ⟨100⟩ axes, that is, parallel to the staircase array of the vicinal surface. However, if a QD is very elongated, its optical properties evolve toward those of a quantum wire; that is, the emission tends to be linearly polarized in a direction parallel to the wire axes. So the polarization

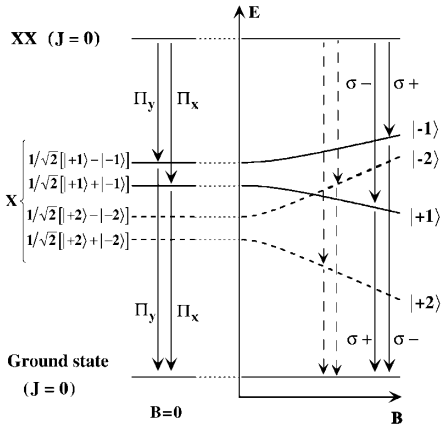

FIG. 4. Schematic illustration of the exciton and biexciton ground states in a zinc blende based QD with reduced symmetry, in zero and nonzero magnetic fields. Solid arrows correspond to the allowed optical transitions. Dark states become observable if a mixing of $|\pm 2\rangle$ and $|\pm 1\rangle$ levels occurs (dotted arrows)

direction of the high intensity component of our exciton doublet corresponds to the main axis of the elongated QD and the intensity difference corresponds to the so called polarization anisotropy [12] calculated by Tanaka *et al.* [13] for a rectangular QD.

The polarization anisotropy is directly related to valence band mixing. More exactly, the difference between the oscillator strength for polarization parallel and normal to a wire axis is proportional to $J_{hh} \cdot J_{lh}$, where J_{hh} (J_{lh}) is the overlap of the electron envelope function with the heavy (light) hole part of the hole envelope function [12]. This means that the observed excitons have a substantial light-hole character as will be confirmed by the magneto-optical measurements. Furthermore, to stress on the importance of valence band mixing in these structures we can note that μ-PL measurements of highly strained asymmetric CdTe QDs in a ZnTe matrix studied in the same setup do not show this polarization anisotropy [14].

Let us consider now the biexciton transitions. Biexciton recombination leaves an exciton X as an intermediate state:

$$\mathrm{XX} \rightarrow \mathrm{X} + h\nu_{xx}\,.$$

Since the biexciton ground state is a spin-singlet state ($J = 0$), the splitting and polarization of line XX are controlled by the structure of the intermediate exciton X. Consequently, as shown in Fig. 4, the energy and intensity sequence of the linearly polarized X and XX transitions shows mirror symmetry in agreement with experimental spectra. As pointed out by Kulakovskii *et al.* [4] for CdSe QDs, this result confirms that the biexciton and the exciton transition take place in the same QD, very strongly elongated in our case.

Figure 3 shows the emission spectra for various magnetic fields applied along the growth axis. To observe the X and XX emission clearly, the spectra were obtained with an excitation power of P_0 and $4P_0$, respectively (P_0 is about 1 W/cm^2). As the magnetic field increases the emission lines show a diamagnetic shift and an additional Zeeman splitting. The two radiative exciton components become progressively circularly polarized. But, even at 8 T the transitions conserve an elliptic polarization. From the Zeeman splitting of the radiative exciton doublet at high fields we obtain an excitonic g factor $g_x = -0.95$. This value is quite different from the value expected in a narrow CdTe quantum well [15] and confirms the mixing of heavy- and light-hole states: Valence band mixing strongly modifies the hole g factors and thus affects the exciton Zeeman splitting [12,16].

At high field, two additional PL lines (X_{dark} in Fig. 3b) appear on each side of the lower component of the radiative doublet X. We attribute these lines to the "dark" exciton states, predominantly made up of the $|\pm 2\rangle$ heavy-hole exciton states. It is well established that in a perfect zinc blende material (Td point group), a magnetic

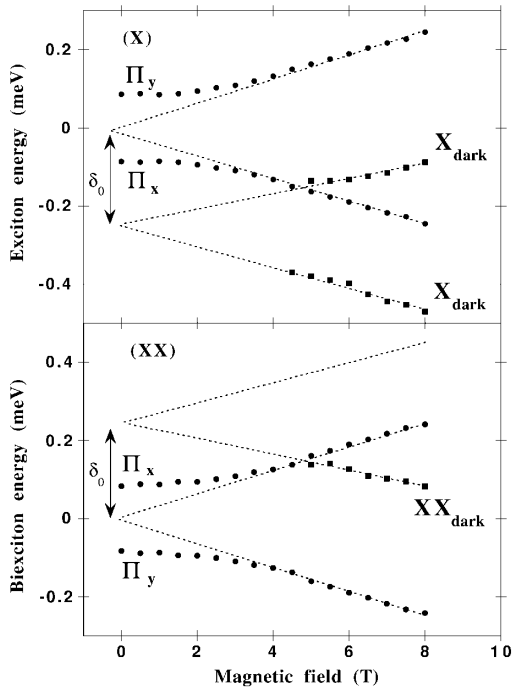

FIG. 5. Magnetic field dependence of the exciton (X) and biexciton (XX) transition energies in the anisotropic island after removing the diamagnetic shift. The centers of the radiative doublets are taken as the reference energy.

field applied along the ⟨100⟩ direction does not mix the heavy-hole exciton states $|\pm 2\rangle$ and $|\pm 1\rangle$ [17,18]. The same is expected for an exciton confined in a quantum well (D_{2d} point group) or localized in an island with D_2 or C_{2v} point group symmetry. So we attribute the optical observation of the dark exciton to the valence band mixing that results from the very asymmetric shape of the island. We note that the observation of the dark exciton in GaAs QDs has also been attributed by Bayer *et al.* [5] to a reduction of the symmetry of the localization potential (to less than C_{2v} or D_2). In the present work, in addition, the presence of the biexciton has allowed us to find a biexciton transition related to the dark exciton states.

As seen in Fig. 3 the biexcitonic and the excitonic transitions show a remarkably similar evolution as the magnetic field increases. The polarization of the biexciton components becomes slightly circular and within the experimental accuracy the doublet splitting is identical to the exciton's (Fig. 5). A third line, labeled XX_{dark}, appears in the PL spectra at the high energy side of XX when X_{dark} grows at the low energy side of X. The transition schemes in Fig. 4 account for this line. Under field conditions where the dark exciton X_{dark} can be detected, the biexciton transition XX_{dark} to this now optically active eigenstate is observed.

As quoted before, the observed levels are not pure heavy-hole exciton states $|\pm 1\rangle$ and $|\pm 2\rangle$ but a mixture of light- and heavy-hole exciton states. However, if we neglect the valence band mixing, the observation of the dark states gives a direct estimate of the isotropic exchange splitting δ_0 between dark and bright states. Assuming the same diamagnetic shift for the $|\pm 1\rangle$ and $|\pm 2\rangle$ sublevels we obtain $\delta_0 = 270\ \mu$eV which is larger than the bulk CdTe value (60 μeV) [19]. This difference shows the strong enhancement of the exchange interaction by the quantum confinement, which in this case is mainly the quantum well potential rather than the lateral potential.

Finally, by extrapolating the lines X_{dark} and XX_{dark} to the zero-field limit (Fig. 5), we find that the difference of biexciton binding energy between the two bright excitons and two dark excitons roughly corresponds to $2\delta_0$. This observation is consistent only with the assumption that the binding of two bright excitons or two dark excitons leads to the same biexciton state. This is the case in the limit of strong confinement. In that limit, the difference of binding energy between the two types of exciton corresponds to their difference of exchange energy, that is, $2\delta_0$.

In summary, we have studied exciton and biexciton states confined in a single elongated island. We have shown that the large asymmetry of the confinement potential causes a large anisotropy of polarization as well as an exchange splitting of the radiative exciton doublet. The biexciton fine structure is found to be fully determined by the exciton's fine structure and, remarkably, we directly observe a biexcitonic line corresponding to a transition to a dark exciton state.

This work is part of the CEA-CNRS joint research program "Nanophysique et Semiconducteurs."

*Corresponding author.
Email address: lbesombes@cea.fr

[1] K. Brunner *et al.*, Phys. Rev. Lett. **73**, 1138 (1994).
[2] D. Gammon *et al.*, Phys. Rev. Lett. **76**, 3005 (1996).
[3] A. Kuther *et al.*, Phys. Rev. B **58**, 7508 (1998).
[4] V. D. Kulakovskii *et al.*, Phys. Rev. Lett. **82**, 1780 (1999).
[5] M. Bayer *et al.*, Phys. Rev. Lett. **82**, 1748 (1999).
[6] H. Mariette *et al.*, Microelectron. J. **30**, 329 (1999); D. Martrou *et al.*, Thin Solid Films (to be published).
[7] D. Martrou *et al.*, Phys. Rev. Lett. **83**, 2366 (1999).
[8] H. Kamada *et al.*, Phys. Rev. B **58**, 16 243 (1998).
[9] E. Blackwood *et al.*, Phys. Rev. B **50**, 14 246 (1994).
[10] E. L. Ivchenko, Phys. Status Solidi (a) **164**, 487 (1997).
[11] J. V. Gupalov *et al.*, JETP **86**, 388 (1998).
[12] U. Bockelmann *et al.*, Phys. Rev. B **45**, 1688 (1992); F. Vouilloz *et al.*, Phys. Rev. B **57**, 12 378 (1998).
[13] T. Tanaka *et al.*, Appl. Phys. Lett. **62**, 756 (1993).
[14] L. Besombes *et al.*, in Proceedings of The Ninth International Conference on II-VI Compounds [special issue J. Cryst. Growth (to be published)].
[15] A. A. Kiselev *et al.*, J. Cryst. Growth **184/185**, 831 (1998).
[16] E. L. Ivchenko *et al.*, JETP Lett. **67**, 43 (1998).
[17] K. Cho *et al.*, Phys. Rev. B **11**, 1512 (1975).
[18] Al. L. Efros *et al.*, Phys. Rev. B **54**, 4843 (1996).
[19] W. Wardzynski *et al.*, Solid State Commun. **10**, 417 (1972).